JOURNAL OF CATALYSIS 129, 216–224 (1991)

Electrocatalytic Conversion of Carbon Dioxide to Methane and Oxygen with an Oxygen Ion-Conducting Electrolyte

TURGUT M. GÜR, HENRY WISE, AND ROBERT A. HUGGINS

Department of Materials Science and Engineering, Stanford University, Stanford, California 94305

Received February 15, 1990; revised July 17, 1990

The performance characteristics of a solid-state electrochemical cell have been examined for the catalytic conversion of carbon dioxide and hydrogen to methane and oxygen. The electrolyte, made up of yttria-stabilized zirconia (YSZ), served the dual function of (a) a support material for the platinum catalyst, and (b) an oxygen ion-conducting membrane for the removal of surface oxygen formed during the reaction. The results indicate a linear increase in reaction rate with DC bias applied across the solid electrolyte. The reaction proceeds by way of a stepwise abstraction of oxygen atoms from carbon dioxide and hydrogenation of surface carbon to methane. The rate-limiting step is found to be the transport of oxygen ions through the solid electrolyte.

I. INTRODUCTION

Metal catalysts in contact with a solid electrolyte support have been used in a number of recent studies for the purpose of oxygen addition to or removal from inorganic and organic parent molecules. Examples of such studies are the partial or complete oxidation of alkanes and olefins (*1, 2*) and reduction of carbon oxides (*3, 4*) CO_x and nitrogen oxides (*5*) NO_x ($x = 1$ or 2). The operating principle common to these reactions is the oxygen ion-conducting property of certain solid electrolytes, which by anodic or cathodic polarization can transport oxygen ions to and from the catalytic surface. A solid electrolyte commonly used for this purpose is cubic zirconia stabilized by the addition of yttria or calcia.

Because of its ability to conduct oxygen ions, the zirconia solid electrolyte can act as a nonporous membrane for the transport of oxygen ions in the presence of an electrical potential difference applied between its electrodes. In particular, electrochemical pumping of oxygen provides a rather interesting technique for driving chemical reactions in a direction far removed from chemical equilibrium, as in the present study which involves the synthesis of methane and oxygen by the reaction with the overall stoichiometry: $CO_2 + 2H_2 = CH_4 + O_2$. Also this reaction is of special interest to the problem of oxygen recovery in life support systems, because it eliminates graphite deposition (*6*) as a troublesome by-product. The electrochemical reactor configuration described in this paper gives only gaseous products, namely, oxygen and methane, that are collected in two separate compartments.

In qualitative terms the process proceeds by way of the following steps: (1) dissociation of carbon dioxide accompanied by transport of oxygen across the solid electrolyte in the presence of an applied field, and (2) rapid hydrogenation of the surface carbon, formed from carbon dioxide, by reaction with hydrogen in the reactor. The surface carbon, formed as a result of the electrochemical abstraction of oxygen from carbon dioxide, is highly reactive toward hydrogen. Its residence time on the metal surface is too short to cause nucleation and growth of graphite. The participation of surface carbon formed by CO or CO_2 dissociation on transition-metal surfaces has been identified previously (*7, 8*) as a critical step in methane formation from synthesis gas.

0021-9517/91 $3.00

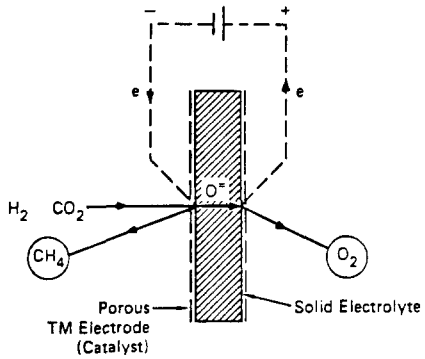

FIG. 1. Schematic diagram of solid-state electrochemical reactor illustrating the abstraction and transport of oxygen through the YSZ solid electrolyte under DC bias.

II. EXPERIMENTAL ASPECTS

The electrochemical reactor configuration shown in Fig. 1 can be represented by

$$(-)\ H_2,\ CO_2,\ Pt/(Y_2O_3)_{0.08}(ZrO_2)_{0.92}/\ Pt,\ air\ (+)$$

At the negative electrode the carbon dioxide is stripped off its oxygen atoms. They are transported as oxygen ions through the yttria-stabilized zirconia (YSZ) solid electrolyte and released as oxygen molecules at the positive electrode. The surface carbon formed on the negative metal electrode is hydrogenated to methane by reaction with hydrogen. At constant applied voltage, the current flowing in the external circuit provides a quantitative measure of the rate of oxygen ion transport during reaction, since YSZ is predominantly an oxygen ion-conducting electrolyte.

The critical component of the electrochemical reactor was a YSZ solid electrolyte tube (1.2 cm in outer diameter), closed at one end and surrounded by an open-ended concentric quartz cylinder (2.2 cm in outer diameter). The reaction gas mixture was recirculated by means of a diaphragm pump through the space between the outer wall of the YSZ tube and the quartz jacket. Porous Pt electrodes were deposited onto the inner and outer walls of the YSZ tube near its closed end by first coating a thin layer of Pt paste (Hanovia No. 6926) and then baking in air at about 800°C. By this means a strongly bound Pt deposit was obtained with geometric surface areas ranging from 8 to 10 cm^2. The outer wall of the Pt-coated YSZ tube served as the catalytic surface. The interior section of the tube was open to the ambient air and the porous Pt electrode served as a reference electrode with fixed oxygen activity.

The reactor system, shown schematically in Fig. 2, had a total internal volume of 115 ml. It contained several zero-dead-volume multiport valves for injecting reactant gases, withdrawing samples for chemical analysis by gas chromatography, and switching reactor operation from continuous flow to recirculation mode. The results reported here were obtained in the recirculating mode.

The quartz cylinder containing the YSZ tube was heated by means of an electric furnace and maintained at the desired temperature with a temperature controller (±2 K). Before each experiment the system was flushed with helium (99.99 vol%) to purge it of all residual gases. Subsequently the helium flow was replaced by a flow of hydrogen (99.99 vol%). After switching to the recirculating mode known quantities of carbon dioxide (99.99 vol%) were injected into the reactor containing hydrogen or mixture of hydrogen and helium. The initial H_2/CO_2 volume ratio in the reaction mixture was selected to be greater than 10. Small aliquots of gas samples (about 0.25 ml in volume) were taken intermittently from the reaction system through a sampling valve and were analyzed on line by a gas chromatograph.

A suitable DC bias larger than the reversible cell potential was imposed across the electrolyte. The current through the cell and the applied voltage were measured continuously during the reaction. A circuit diagram is presented in Fig. 3. In the evaluation of the experimental results the pumping poten-

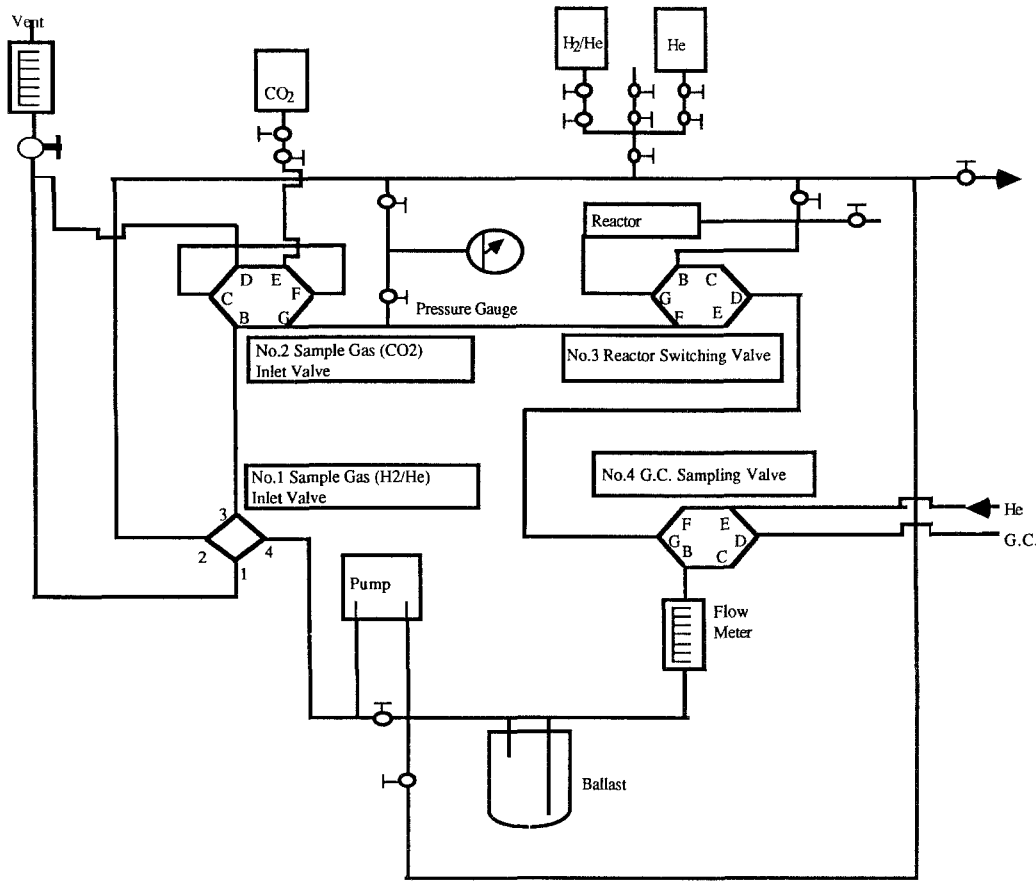

FIG. 2. Schematic details of experimental apparatus showing the electrochemical reactor and analytical system. The four-port valve allows switching between continuous flow and recirculating modes. The three six-port valves are used for reaction mixture preparation and sampling for gas chromatographic (GC) analysis.

tial E_p was used as one of the parameters. It represents the driving force for oxygen ion transport and is given by the difference between the applied potential and the open-circuit potential

$$E_p = E_{appl} - E_{oc}.$$

It should be noted, however, that the pumping potential contains two additional terms, (a) the ohmic overpotential caused by the finite resistances of the electrolyte and the electrodes, and (b) the activation overpotentials at the anode and the cathode resulting from the finite rate of charge transfer at the electrode/electrolyte interfaces.

III. EXPERIMENTAL RESULTS

A. Chemical and Electrochemical Measurements

The experiments were carried out under potentiostatic (i.e., constant voltage) conditions. The parameters under study included the applied potential, reaction temperature, and reactant composition. The time-dependent variation of the chemical composition of the reaction system at 973 K and a pumping potential of 1.0 volt is shown in Fig. 4.

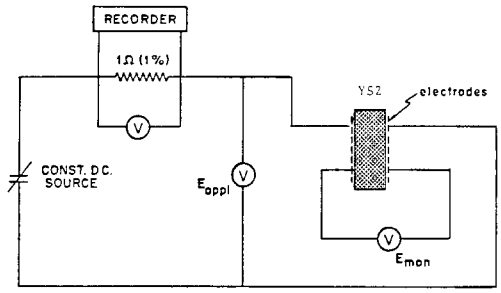

FIG. 3. Schematic circuit diagram for electrochemical measurements under potentiostatic mode.

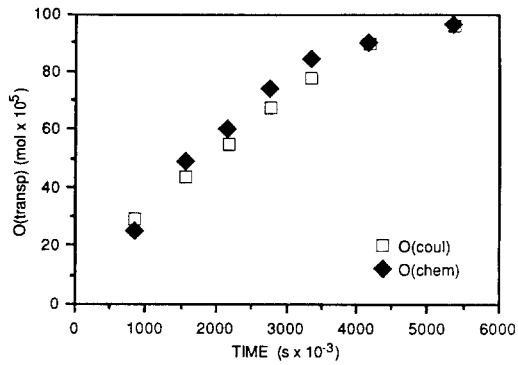

FIG. 5. Oxygen ion-transport rate through the reactor operating at 1073 K and a pumping potential of 1.0 V (initial CO_2 = 48 × 10^{-5} mol).

The curves demonstrate the progress of the reaction as monitored by sampling of the gas composition as a function of reaction time. It can be seen that in the region of relatively rapid disappearance of carbon dioxide the formation of carbon monoxide far exceeds that of methane. However, as the carbon monoxide concentration passes through a maximum, the rate of build-up of methane in the reactor becomes quite pronounced. This reaction pattern was observed in all the measurements performed over a temperature range from 873 to 1173 K and pumping potentials ranging from 0.5 to 2.0 V.

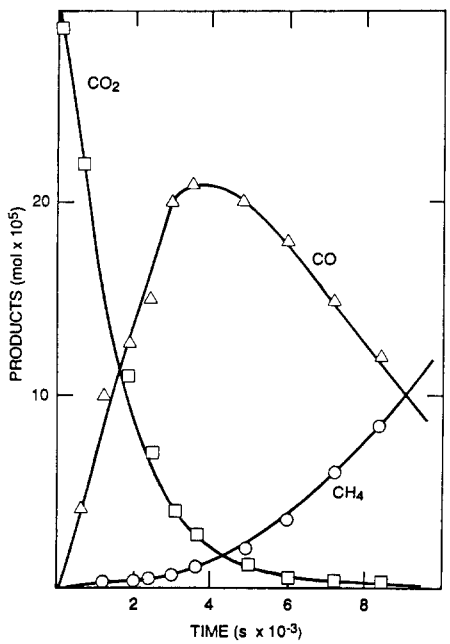

FIG. 4. Variation of gas composition during reaction in recirculating reactor at 973 K and a pumping potential of 1.0 V.

During reaction each molecule of CH_4 formed by the reduction of CO_2 involves the removal of two oxygen atoms. For the case of CO it involves the removal of one oxygen atom. Thus, in terms of an oxygen mass balance the total amount of oxygen transported through the electrolyte is equivalent to the molar sum of $2n_{CH_4} + n_{CO}$, where n denotes the number of moles of product formed. On this basis, the coulometric measurements can be compared with the chemical determinations. The agreement between the data (Fig. 5) at 873 K and a pumping potential of 1.0 V demonstrates the validity of such a correlation within the experimental error of ±5%. Similarly, the results of the coulometric and chemical measurements obtained at 1173 K and an applied potential of 2.0 V, shown in Fig. 6, concur within the experimental error.

B. Analysis of Reaction Kinetics and Mechanism

In order to interpret the reaction kinetics it is necessary to consider a reaction mechanism involving the following steps for the reduction of CO_2 to CH_4,

$$CO_2 \xrightarrow{k_1} CO + O(a) \qquad (1)$$

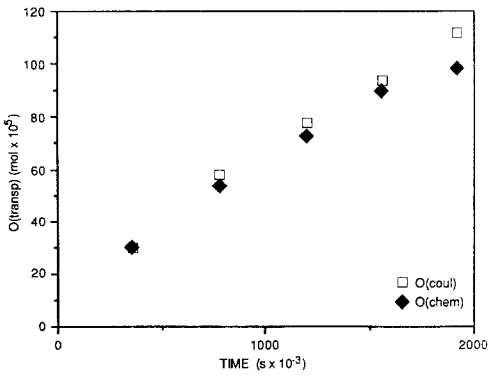

FIG. 6. Oxygen ion-transport rate through the reactor operating at 1073 K and a pumping potential of 2.0 V (initial $CO_2 = 9 \times 10^{-5}$ mol).

$$CO(a) \xrightarrow{k_2} C(a) + O(a) \qquad (2)$$

$$C(a) + H(a) \xrightarrow{k_3} CH(a) \rightarrow \ldots \rightarrow CH_4, \qquad (3)$$

where k_1, k_2, and k_3 represent the rate constants for each of the reactions listed. In reaction (3), stepwise hydrogenation of surface carbon is postulated in accordance with published studies on surface carbon removal from transition metals. The oxygen atoms formed in steps (1) and (2) are transported as oxygen ions through the solid electrolyte. This process involves first the interaction of oxygen atoms with anion vacancies and electrons at the negative electrode [$O(a) + V_0^{\cdot\cdot} + 2e^- = O_0^x$]. The oxygen ions are transported through the YSZ electrolyte and converted at the positive Pt electrode to neutral oxygen atoms by the reverse of the reaction shown above. They desorb after recombination to oxygen molecules. By this process the oxygen molecules are separated from the reaction chamber and do not participate in any further chemical reaction.

Based on this reaction model a kinetic analysis is performed that describes the time-dependent disappearance of reactants and formation of stable products. Details of the derivation are to be found in the Appendix. In the presence of excess hydrogen, as is the case in our experiments, the variations with time of the CO_2 and CO concentrations during the course of an experiment are given by

$$[CO_2] = [CO_2]_0 \exp\{-k_1 t\} \qquad (4)$$

and

$$[CO] = \{k_1 [CO_2]_0/(k_2 - k_1)\} \{\exp(-k_1 t) - \exp(-k_2 t)\}, \qquad (5)$$

where the quantities in the square brackets represent molar concentrations, the parameter t the reaction time, k_1 and k_2 the rate constants for reactions (1) and (2), and the subscript zero the initial conditions ($t = 0$).

The carbon monoxide kinetics described by Eq. (5) exhibit a maximum at $t = t_m$, at which

$$d[CO]/dt = 0 = k_1 \exp(-k_1 t_m) + k_2 \exp(-k_2 t_m). \qquad (6)$$

Thus, by measuring the exponential decay in $[CO_2]$ as given by Eq. (4) one obtains the rate constant k_1. From the location of the maximum in [CO] at $t = t_m$ one calculates the rate constant k_2, as specified by Eq. (6).

C. Evaluation of Rate Constants

Calculations of the rate constants k_1 and k_2 by the procedure just presented have been made for a range of temperatures and pumping potentials. They are plotted in accordance with the Arrhenius equation in Figs. 7 and 8. The experimental error in the rate constants is estimated to be ±15%. Based on these data one obtains an activation energy of 62 ± 10 kJ mol^{-1} for reaction (1) and 65 ± 10 kJ mol^{-1} for reaction (2) for pumping potentials of < 2.0 V. Within the experimental error the activation energies for both reactions are identical. But the individual rate constants for reactions (1) and (2) differ considerably, because the activation entropy, expressed as the preexponential term in the Arrhenius equation is greater by a factor of 15 for removal of an oxygen atom from CO_2 (reaction (1)) than from CO (reaction (2)).

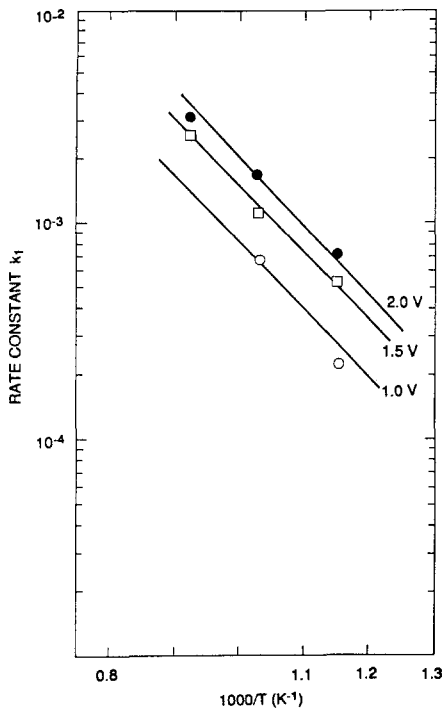

FIG. 7. Variation of rate constant k_1 with temperature at different pumping voltages.

Of interest is not only the variation of the measured rate constants with temperature at constant potential, but with pumping potentials under isothermal conditions. For this comparison the rate constants k_1 and k_2 at 1000 K were selected by interpolation of the data exhibited in Figs. 7 and 8. It is apparent that both rate constants k_1 and k_2 show a linear increase with pumping voltage up to about 2.2 V. At higher pumping voltages the experimental rate constants begin to deviate from linearity because the decomposition potential of the electrolyte is exceeded (Fig. 9).

IV. DISCUSSION

The experimental results demonstrate the feasibility of reducing carbon dioxide in the presence of hydrogen to oxygen and methane. The two products are separated from each other by means of the solid electrolyte cell. The carbon deposition problems encountered in earlier work (*3*) is mitigated by the rapid conversion of surface carbon species to methane on the metal catalyst in contact with the oxygen ion-conducting YSZ solid electrolyte. With Pt as the catalyst electrode, the contribution of an applied electrical potential to the reaction rate is particularly pronounced, since in its absence no methane formation is detectable within the limits of our measurements. This behavior is not unexpected because platinum is a relatively poor catalyst for dissociative adsorption of carbon dioxide or carbon monoxide, an essential step in methane synthesis from syngas.

In earlier studies with YSZ, the influence of applied potential on the catalytic properties has been established. Large enhancements in reaction rates (*1–5, 9–12*) and significant changes in selectivities (*10, 11*) have been reported for various heterogeneous reactions on different catalyst electrodes. In

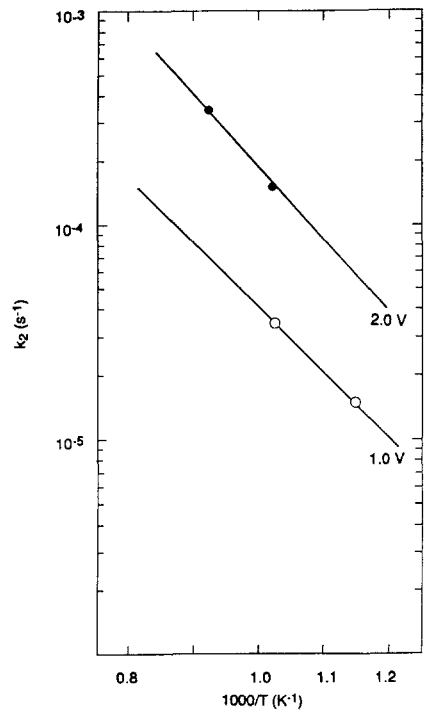

FIG. 8. Variation of rate constant k_2 with temperature at different pumping voltages.

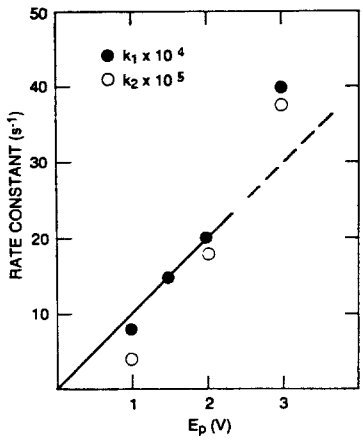

FIG. 9. Effect of pumping voltage on rate constants.

most cases, the observed enhancements in reaction rates were faradaic in nature; i.e., the catalytic rate was determined by the rate of oxygen transport through the solid electrolyte.

The linear dependence of the rate constants k_1 and k_2 on pumping voltage (Fig. 9) and the good correlation observed between the coulometric and chemical measurements at voltages below the decomposition potential of YSZ provide information on the electrical behavior of the solid electrolyte during the catalytic reaction. Because of the nonsteady-state conditions prevailing in the recirculating reactor, the electrical current measurements made under potentiostatic conditions reflect the continuous changes in oxygen formation and transport rate during the chemical reaction. Therefore, the rate constants rather than the rates are a more satisfactory measure of the reaction kinetics. Their linear variation with the pumping voltage, as shown in Fig. 9, is a strong indication of ohmic impedance during chemical reaction. The results preclude the contribution of rate-controlling electrode reactions and point to oxygen ion transport as the slow step in the overall process. The activation energies measured for oxygen removal from carbon dioxide and carbon monoxide are identical and nearly equal to the activation energy for oxygen ion transport in zirconia (*20*) (70 kJ/mol). Thus, it can be concluded that the rate-limiting step is the oxygen ion transport through the solid electrolyte and not the splitting of the C-to-O bond nor the hydrogenation of surface carbon to methane. The pumping potential enhances the overall chemical reaction rate by increasing the oxygen ion transport rate through the electrolyte.

Based on the results obtained at 973 K, one calculates a transport rate for oxygen ions through the solid electrolyte of 1.6×10^{-4} mol m^{-2} s^{-1} at a pumping potential of 1 V for a reactant gas mixture containing initially 23 vol% CO_2 and 77 vol% H_2 at a total pressure of 1 atm. The simultaneous production of gaseous methane corresponds to a turnover frequency of 20 s^{-1}.

When the decomposition potential of zirconia is exceeded, the coulometric data no longer conform to but exceed the chemical measurement of oxygen ion transport. Removal of lattice oxygen and reduction of solid zirconia electrolyte start to occur under these conditions. This process is accompanied by the formation of additional oxygen anion vacancies and electrons that form a semiconducting region on the YSZ surface in the vicinity of the three phase boundary. Reportedly high reactivity (*5, 15, 17, 18*) of this region may cause the abrupt increase in the rate constants at pumping potentials in excess of the decomposition potential of the YSZ solid electrolyte. As the decomposition progresses with time, the semiconducting surface region proceeds from the cathode toward the anode and eventually causes internal shorting of the solid electrolyte. Under these circumstances, the current measured is no longer predominantly ionic, but electronic conduction makes a significant contribution to the total conductivity. Also, the mass balances for carbon and oxygen turn unsatisfactory because of carbon accumulation at the negative electrode in the form of graphite. The graphite formed is relatively inactive to reaction with hydrogen as compared to surface carbon.

Recently, Vayenas and co-workers (*14,*

15) reported nonfaradaic effects in electrocatalytic oxidation studies of several organic compounds using YSZ electrolyte provided with different types of metal electrodes. They concluded that the applied electrical potential modifies the work function of the positive catalyst electrode, and thereby the binding of the adsorbed species (*16*). The results of our study, involving CO_2 reduction at the negative electrode, do not show any evidence for such nonfaradaic behavior.

APPENDIX: MATHEMATICAL ANALYSIS OF REACTION KINETICS

A kinetic model for the catalytic reduction of carbon dioxide to methane is based on the three reaction steps given earlier (see text), in which stepwise removal of oxygen atoms from carbon dioxide is followed by hydrogenation of surface carbon. With k_1 the rate constant for the catalytic reduction of carbon dioxide to monoxide and k_2 the rate constant for reduction of carbon monoxide to carbon, one obtains

$$-d[CO_2]/dt = k_1[CO_2] \quad (1)$$

$$-d[CO]/dt = k_2[CO] - k_1[CO_2]. \quad (2)$$

The rate for the formation and removal of carbon reads

$$-d[C]/dt = k_3[C] - k_2[CO]. \quad (3)$$

Finally, the rate of methane formation is governed by

$$d[CH_4]/dt = k_3[C]. \quad (4)$$

Because the experiments described were carried out in the presence of a large excess of gaseous hydrogen, the rate equation (4) is considered to be independent of hydrogen pressure.

In accordance with reaction (1), the concentration of carbon dioxide decreases exponentially with time, so that a plot of the natural logarithm of $[CO_2]$ against time yields a straight line with slope $[-k_1]$. The concentration of carbon monoxide passes through a maximum as specified by reaction (2). At the maximum

$$d[CO]/dt = 0$$

so that, by Eq. (2),

$$k_2 = k_1\,[CO_2]/[CO].$$

Solution to the differential equations may be obtained by using the initial values, at $t = 0$,

$$[CO_2] = [CO_2]_0 \quad \text{and} \quad [CO] = [C] = [CH_4] = 0$$

after integration one obtains

$$[CO_2] = [CO_2]_0 \exp(-k_1 t)$$

and

$$[CO] = A\,[\exp(-k_2 t) - \exp(-k_1 t)],$$

with $A = k_1[CO_2]_0/(k_1 - k_2)$.

For the variation of [C] and $[CH_4]$ with reaction time the rate equations read

$$[C] = Ak_2\,\{[1/(k_3 - k_1)]\,[\exp(-k_3 t) - \exp(-k_1 t)] + [1/(k_3 - k_2)]\,[\exp(-k_2 t) - \exp(-k_3 t)]\}$$

and

$$[CH_4] = -Ak_2k_3\,\{(1/k_3)\,\{(1/k_1) - (1/k_2)] + [1/(k_3 - k_1)]\,[(1/k_3)\exp(-k_3 t) - (1/k_1)\exp(-k_1 t)] + [1/(k_3 - k_2)]\,[(1/k_2)\exp(-k_2 t) - (1/k_3)\exp(-k_3 t)]\}.$$

ACKNOWLEDGMENTS

This work was sponsored in part by the Office of Naval Research and the Gas Research Institute. Their support is gratefully acknowledged. Mr. T. Nohmi provided valuable assistance in the experimental work.

REFERENCES

1. Stoukides, M., *Ind. Eng. Chem.* **27,** 1745 (1988).
2. Stoukides, M., and Vayenas, C. G., *J. Catal.* **69,** 18 (1981); *J. Electrochem. Soc.* **131,** 839 (1984).
3. Gür, T. M., and Huggins, R. A., *Science* **219,** 967 (1983).
4. Gür, T. M., and Huggins, R. A., *J. Catal.* **102,** 443 (1986).
5. Gür, T. M., and Huggins, R. A., *J. Electrochem. Soc.* **126,** 1067 (1979).
6. Weissbart, J., Smart, W. H., and Wydeven, T., *Aerosp. Med.* **40,** 136 (1969).
7. Wentrcek, P. R., Wood, B. J., and Wise, H., *J. Catal.* **43,** 363 (1976).
8. Araki, M., and Ponec, V., *J. Catal.* **44,** 439 (1976).

9. Michaels, J. N., and Vayenas, C. G., *J. Catal.* **85,** 477 (1984).
10. Farr, R. D., and Vayenas, C. G., *J. Electrochem. Soc.* **126,** 1478 (1980).
11. Yentekakis, I. V., and Vayenas, C. G., *J. Electrochem. Soc.* **136,** 996 (1989).
12. Gür, T. M., and Huggins, R. A., *Solid State Ionics* **5,** 563 (1981).
13. Etsell, T. H., and Flengas, S. N., *Chem. Rev.* **70,** 339 (1970).
14. Bebelis, S., and Vayenas, C. G., *J. Catal.* **118,** 125 (1989).
15. Neophytides, S., and Vayenas, C. G., *J. Catal.* **118,** 147 (1989).
16. Vayenas, C. G., Bebelis, S., and Ladas, S., *Nature* **343,** 625 (1990).